RSC Advances

PAPER

View Article Online
View Journal | View Issue

Cite this: *RSC Adv.*, 2021, **11**, 38047

Effect of a modified 13X zeolite support in Pd-based catalysts for hydrogen oxidation at room temperature

Younghee Jang,[a] Sang Moon Lee*[ab] and Sung Su Kim *[b]

Received 24th August 2021
Accepted 8th November 2021

DOI: 10.1039/d1ra06395b

rsc.li/rsc-advances

This study investigated the effect of a modified 13X zeolite to Pd/zeolite catalyst on the oxidation of hydrogen to ensure safety from hydrogen leakage. The catalytic activity of Pd/zeolite catalysts was significantly affected by acid treatment of 13X zeolite support and various calcination temperatures (300 °C, 400 °C, 500 °C, 600 °C) of the Pd/zeolite catalyst. To understand the correlation between the activity and physical properties of the catalysts, activity test, XRD, BET, TEM, TPR, and TPO were performed; Pd/13X (400) was shown to have a high catalytic activity, which depended on the dispersion and particle size of palladium. Also, a strong PdH on the catalyst surface was formed, and a high catalytic activity at a low hydrogen concentration was obtained.

1. Introduction

Hydrogen is a clean energy source that does not generate pollution and has the highest calorific value (150 kJ kg^{-1}) among fuels. Recently, policies have emerged to actively utilize hydrogen as a fuel. In particular, hydrogen can be produced from various hydrogen-containing fuels and can be stored in various forms, which enables stable transportation.[1–3] Currently, hydrogen vehicles exemplify the successful commercialization of hydrogen fuel. Therefore, numerous companies are actively looking to enter the hydrogen vehicle market. In addition, hydrogen fuel applications are expanding to all means of transportation, including in industrial[4] and household electricity,[5] ships,[6] and railways.[7,8] Despite these advantages, people are reluctant to use hydrogen in daily life owing to its low volumetric density and safety. In particular, it exhibits explosive properties at a concentration of 4% or higher, which may lead to critical safety issues due to hydrogen leakage.[9–11] Owing to its low molecular weight and rapid diffusion, a ventilation system is used as the main safety device in most technologies. However, an unexpected safety accident, such as sudden failure of ventilation in a closed space, such as underground, may lead to concentration of hydrogen, and therefore, cause explosion. So, strong safety systems must be in place to prevent such accidents and enable the stable and steady use of hydrogen energy. Room-temperature catalysis, widely employing noble metal catalysts, such as platinum and palladium, is applied to prevent hydrogen leakage at room temperature.[9–13] In this technique, unlike the gas oxidation reaction, which has excellent efficiency as the target concentration is lower, the reaction becomes more active as the hydrogen concentration increases. Also, a lot of research showed that the noble metal catalyst was dispersed in the form of nano particles on the support. However, the uniform dispersion of Pd is very challenging in the context of heterogeneous catalysts.[14–16] Therefore, to overcome the limitations of noble metal nanoparticles, a reducing support capable of expressing the SMSI effect is used to help to highly disperse Pd. Owing to the low pressure drop of the honeycomb catalyst, Uda *et al.* proposed it as an alternative to the existing particle catalysts.[17] The exothermic reactions and catalyst deactivation due to the product (water) are the most representative catalyst performance degradation factors. Therefore, studies related to catalyst performance need to be conducted. Iwai *et al.* confirmed the performance of Pt catalysts, which could remove tritium in a nuclear power plant under water vapor partial pressure conditions.[18,19] Lomot *et al.* found that the catalyst performance of the Pt/Al_2O_3 catalyst was significantly reduced with the production of water, but it regenerated on drying.[20] Most studies focused on the influence of water, but the studies on the physical properties of the catalyst and their reaction activities are required. Recently, catalyst studies using a Pt–Pd bimetal as an active metal have been reported. An oxidation performance of 99.9% or more was confirmed at 1% hydrogen concentration using a Pd–Pt catalyst by Kim *et al.*[21] Tanaka *et al.* showed hydrogen or methane oxidation performance using a Pd–Pt catalyst, and the hydrogen conversion was 100% at 100 °C.[22] However, to date, no study has confirmed the activity of catalysts at both low hydrogen concentrations of less than 0.5% and high hydrogen concentrations of 2% or higher.

[a]*Department of Environmental Energy Engineering, Graduate School of Kyonggi University, 154-42, Gwanggyosan-ro, Yeongtong-gu, Suwon-si, Gyeonggi-do, Korea*
[b]*Department of Environmental Energy Engineering, Kyonggi University, 154-42, Gwanggyosan-ro, Yeongtong-gu, Suwon-si, Gyeonggi-do, Korea. E-mail: sskim@kyonggi.ac.kr*

Particularly, all catalytic activities at low hydrogen concentrations of less than 0.5% are extremely low.[22–25] Lalik *et al.* investigated the Pd–Au catalyst activity under various hydrogen concentration conditions and found that when the injected hydrogen concentration was high, there was a decrease in the catalyst activity for hydrogen removal because of the exothermic reaction.[26,27] When hydrogen is oxidized, the temperature of the catalyst rises due to the heat generated. This increases the size of the Pd nano particles in the catalyst and becomes one of the causes of decreasing the activity. Consequently, it is a necessary to develop a catalyst that overcomes all performance degradation factors (high heat or low hydrogen concentration). Zeolite is a suitable support for answering that question. It has a certain frame made of Si and Al. Among them, 13X zeolite is a hydrophilic support with a Si/Al ratio close to 1, that is, strong H_2O adsorption. It is economical and easy to obtain among zeolites. However, as hydrogen oxidation is a reaction, in which water is produced, moisture in the catalyst cannot escape and is adsorbed on the catalyst. Therefore, it is necessary to try small hydrophobization by increasing the Si/Al ratio of the 13X zeolite and study to increase the H_2 oxidation rate. Silaghi *et al.* observed the mechanism of Al species during dealumination considering the zeolite framework.[28] Luo *et al.* tried to hydrophobize the hydrophilicity of a zeolite using an acidic treatment.[29] Numerous researchers are trying to make zeolites hydrophobic by controlling the Si/Al ratio, and they are proving the effect. However, studies comparing the hydrogen oxidation performance in various concentration ranges and considering high dispersion using a zeolite support are still poor. In this study, we developed a catalyst with a high oxidation performance at a low hydrogen concentration of less than 0.5%. Palladium with high dissociative hydrogen adsorption was used and a zeolite support with thermal durability for the exothermic reaction was applied for this preparation. The oxidation performance of the as-prepared Pd/zeolite catalyst was confirmed at hydrogen concentrations ranging from 0.3–4%, *i.e.*, below the explosive hydrogen concentration. In addition, the performance influencing factors, such as surface characteristics and the dispersion degree of catalysts, were determined using X-ray diffraction (XRD), Brunauer–Emmett–Teller (BET) model, temperature-programmed reduction (TPR), temperature-programmed oxidation (TPO), chemisorption, and transmission electron microscopy (TEM). Finally, the noble metal content was determined according to the hydrogen concentration by varying the Pd content, so that the catalyst could have economic feasibility.

2. Results and discussion

2.1. Synthesis and characterization of the Pd/13X zeolite

Fig. 1 shows the results of the XRD analysis, which was performed to determine the 13X zeolite structure about acidic treatment or calcination. The XRD patterns of the 13X zeolite were found at 6.2°, 15.6°, 20.1°, 23.3°, 26.7°, and 31°.[30,31] The structure of the 13X zeolite could be found in the acid-treated modified zeolite, but not found after calcination. So, an acidic treatment did not change the XRD pattern of the existing 13X zeolite. However, the sharpness of the structure decreased, and the structure of 13X zeolite disappeared, when it was heat treated.

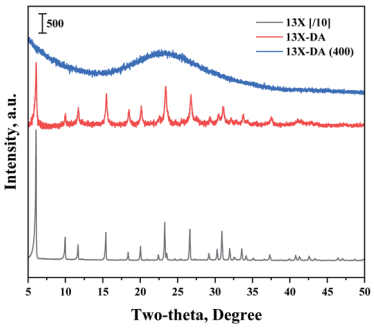

Fig. 1 XRD patterns of 13X and 13X-DA.

Fig. 2 shows the results of the XRD analysis, which was performed to determine the catalyst structure prepared to confirm the effects of the improved hydrogen oxidation performance when the modified zeolite was used. The unique peaks corresponding to 13X zeolite appeared at 6.2°, 15.6°, 20.1°, 23.3°, 26.7°, and 31°.[30,31] The structure of the 13X zeolite could not be confirmed in the acid-treated modified zeolite, and only the peaks corresponding to the active Pd were observed. In the case of the unmodified 13X zeolite catalyst, however, only the 13X zeolite structure was confirmed, while XRD peaks corresponding to the Pd metal were not clearly observed. Alshahidy *et al.* succeeded in enhancing the Si/Al ratio by an acidic treatment of the 13X zeolite and reported that the crystal structure of the zeolite changed according to the acidic treatment.[32] Therefore, the XRD analysis showed that the acidic treatment process disrupted the 13X zeolite structure.

Fig. 3 exhibits the results of the catalyst structures according to the heat-treatment temperatures of the modified zeolite catalysts. Consequently, the intensities of the peaks for the Pd crystals gradually increased on increasing the heat-treatment temperature. In particular, the peaks corresponding to the Pd crystals were very sharp in the catalyst treated at 600 °C, which indicated the crystallization of Pd due to agglomeration on increasing the heat-treatment temperature. Therefore, it was

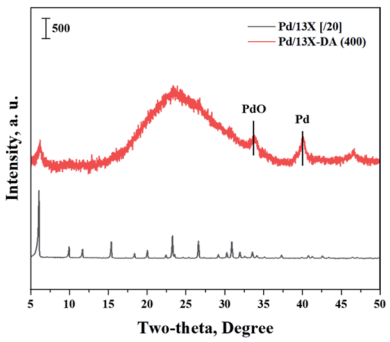

Fig. 2 XRD patterns of Pd/13X and Pd/13X-DA (400).

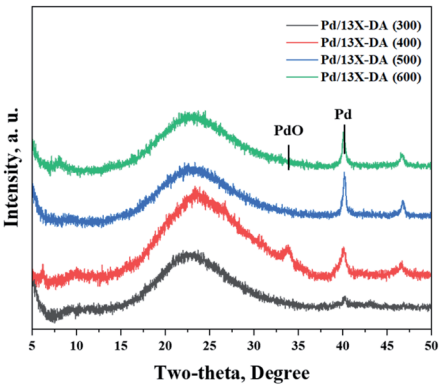

Fig. 3 XRD patterns of 13X zeolite modification over various calcination temperature.

shown that the heat-treatment conditions affected the performance.

BET analysis was performed to determine the specific surface area of the catalyst (Table 1). The pore sizes were similar. However, the pore volumes increased, and the specific surface areas decreased on increasing the temperature. Regardless of dealumination, the catalysts exhibited approximately twice the specific surface areas at 400 °C. Therefore, it was confirmed that the heat treatment at 400 °C was required to properly coat palladium. H_2-chemisorption analysis was performed to confirm the dispersion degree and the size of the Pd metal. The specific area of the as-prepared catalyst was independent to the dispersion degree of the noble metal, but the dispersion degree of metallic Pd increased based on the modification method of the 13X zeolite. Burris *et al.* (2016) reported the improved micropores with a diameter of 10 nm or smaller in the acid-treated zeolites.[33] Both the Pd/13X zeolite catalyst and Pd/13X-DA (400) had a specific area of 37 $m^2\ g^{-1}$ or more. However, only the Pd/13X-DA catalyst with the modified zeolite support exhibited an improved metal dispersion degree, while the unmodified Pd/13X zeolite catalyst exhibited only a 1.7% metal dispersion degree. This was similar to the aforementioned results. Based on this analysis, it was confirmed that the structural specific surface areas of zeolites did not exhibit a significant correlation, but the dispersion degree and size of the metallic Pd significantly influenced the hydrogen oxidation.

2.2. Catalytic properties of the Pd/13X zeolite

H_2-TPR and H_2-TPO analyses were performed in the temperature range of 40–600 °C (Fig. 4 and 5) to confirm the hydrogen oxidation performance of the modified catalysts. A negative peak was found at 80 °C or 84.8 °C. The desorption peaks probably corresponded to the PdH decomposition because Pd has the ability to form hydride phases under normal conditions.[34–37] The catalyst modified at 400 °C exhibited the highest negative value, suggesting the highest oxidation ability. In addition, the unmodified zeolite catalyst prepared at 400 °C exhibited the lowest negative value, suggesting a relatively low hydrogen oxidation ability. These results agreed with the previously confirmed hydrogen conversion performance. Fig. 4 exhibits the H_2-TPO analysis that confirmed the oxidation state by reacting with O_2/N_2 gases after sufficiently adsorbing H_2. Therefore, the hydrogen in the catalyst was not adsorbed and reacted completely because the oxygen molecules were already bound to the catalyst reacted with H_2, which occurred owing to the behavior of the hydrogen oxidation at room temperature. This was confirmed because most of the modified zeolite catalysts with excellent hydrogen oxidation ability did not exhibit a signal or a negative value. In addition, the general zeolite catalysts, with poor hydrogen oxidation ability, exhibited a positive value. It was confirmed that the as-prepared catalyst was highly dispersed as small particles on the catalyst surface when Pd was supported on the modified zeolite. The catalyst modified at 400 °C exhibited the highest dissociative hydrogen adsorption ability. Owing to these characteristics, excellent reaction activity was exhibited in the low hydrogen

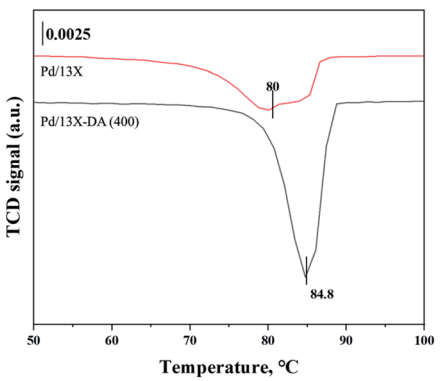

Fig. 4 H_2 consumption profiles during TPR of Pd/13X and Pd/13X-DA (400).

Table 1 The SBET and metallic surface area of the Pd/zeolite catalysts

Catalysts	Surface area ($m^2\ g^{-1}$)	Pore volume	Pore radius (nm)	Metal dispersion	Metallic surface area ($m^2\ g^{-1}$)	Active particle diameter (nm)
Pd/13X	38	0.086	19.1	1.7	0.08	64.4
Pd/13X-DA (300)	19	0.087	19.0	5.6	0.25	20.0
Pd/13X-DA (400)	39	0.080	19.2	7.6	0.34	14.8
Pd/13X-DA (500)	28	0.098	19.0	10.4	0.46	10.8
Pd/13X-DA (500)	24	0.090	19.1	4.6	0.20	24.6

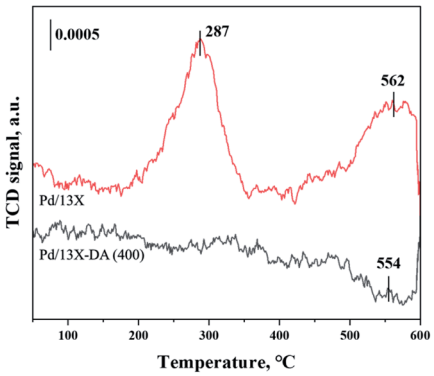

Fig. 5 H_2 oxidation profiles during TPO of Pd/13X and Pd/13X-DA (400).

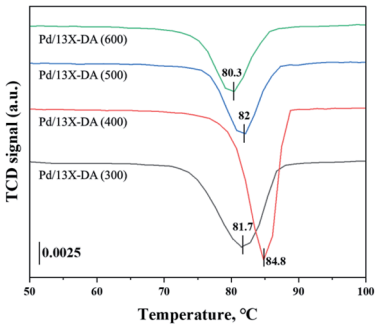

Fig. 7 H_2 consumption profiles during TPR of the 13X zeolite modification over various calcination temperatures.

concentration reaction. Moreover, the TPOR value of the unmodified general zeolite catalyst was smaller than that of other catalysts.

TEM and H_2-chemisorption analyses were performed to identify the causes of the differences in the catalyst effectiveness, and the results are exhibited in Table 1 and Fig. 6. All catalyst particles were uniformly distributed in the samples. The average sizes of the active metals formed on the catalyst surfaces were calculated using TEM analysis. The results: Pd/13X-DA (400) > Pd/13X-DA (300) > Pd/13X-DA (500) > Pd/13X-DA (600) suggested that the dispersion degree and metallic sizes could be controlled during the heat treatment step. Fig. 7 shows the H_2-TPR analysis according to the heat-treatment temperatures of the modified zeolite catalysts. As previously analyzed, Pd, an active metal, reacts with hydrogen at room temperature. It was confirmed that PdH was bound through the H_2-TPR analysis. In addition, relatively large peaks can be observed at 400 °C and 500 °C. In addition, as the size of the active metal decreased, it moved to the right. Similarly, the catalyst prepared at 400 °C was prepared with the smallest active metal size, and after that, it could be determined that the size was smaller in the order of Pd/13X-DA (400) > Pd/13X-DA (300) > Pd/13X-DA (500) > Pd/13X-DA (600). However, it is slightly different from the analysis of H_2 chemisorption, which may be an error due to adsorption in the analysis of the H_2 chemisorption.

2.3. Efficiency of the Pd/13X zeolite

An acidic treatment, which is a modification method that increases the Si/Al ratio by removing Al from the 13X zeolite and is a representative hydrophobic treatment method for zeolites, was used. Hydrophobic zeolites can control the acid strength and suppress the adsorption of H_2O, which is one of the causes of the catalyst deactivation. Numerous researchers reported that the adsorption of H_2O can be controlled by an acidic treatment on various zeolite supports.[23,38–40]

Therefore, in this study, we intended to lower the adsorption of H_2O and enhance the dissociative hydrogen adsorption in the process of highly dispersing Pd on the zeolite. The effects of the support modified by the acidic treatment modification method, which is a zeolite hydrophobic treatment method, are shown in Fig. 8. As a result, it exhibited a hydrogen oxidation capacity of 95% or higher at a low hydrogen concentration (0.3%), while maintaining 100% oxidation performance even at a high hydrogen concentration.

On comparing the catalyst performances of the zeolite catalysts modified (Fig. 9), the performance of the modified catalyst was found to be superior. Therefore, it was shown that the heat-treatment conditions affected the performance. In particular, a heat treatment at 400 °C compared to that at 300 °C

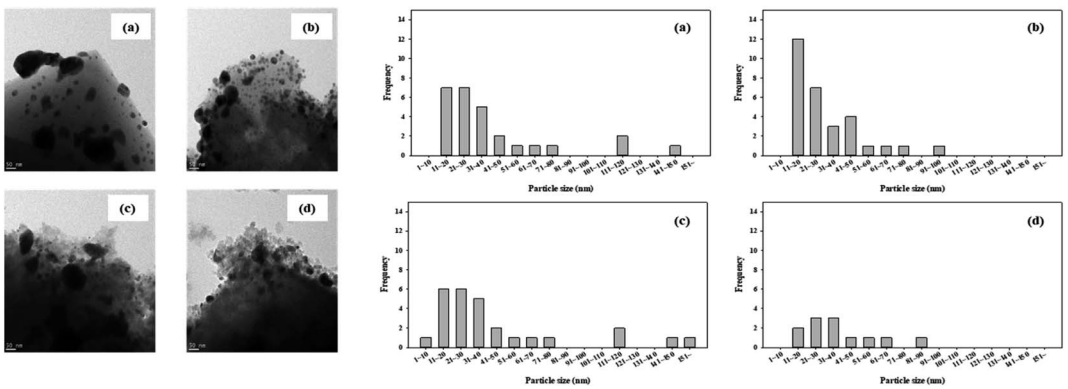

Fig. 6 TEM analysis results of the zeolite catalysts (a) Pd/13X DA(300); (b) Pd/13X DA(400); (c) Pd/13X DA(500); (d) Pd/13X DA(600).

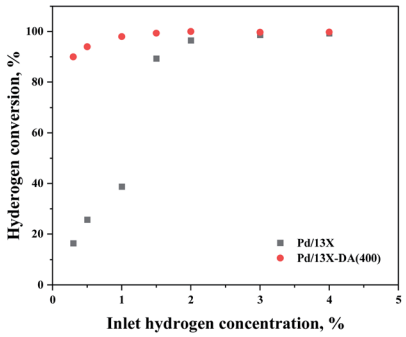

Fig. 8 Effect of the modification over the Pd/13X zeolite catalysts.

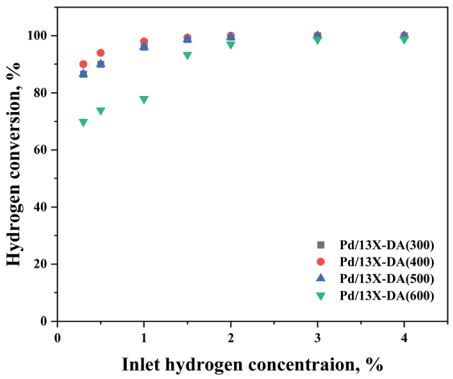

Fig. 9 Effect of the 13X zeolite modification over various calcination temperatures.

did not show a significant difference in the performance, so it was considered as the optimal heat treatment for the catalyst. However, the oxidation performance of the catalyst did not improve with the heat treatment at a relatively high temperature of 600 °C. It was assumed that agglomeration of the active metals occurred at the heat treatment temperature increased to 600 °C. Therefore, an appropriate catalyst heat treatment condition was required.

3. Experimental

3.1. Materials and reagents

The materials and reagents and reagents in this study were obtained from the following sources: 13X zeolite (Si/Al ratio = 1.61, China); palladium chloride ($PdCl_2$), Fisher Scientific; hydrochloric acid solution, 35.0–37.0% (HCl), Samchun.

3.2. Catalyst preparation

Zeolite-based Pd catalysts were developed to maximize the performance and durability of the catalyst at various hydrogen concentrations. 13X zeolite was used (Si/Al = 1.61), and hydrophobic modification was performed to increase the resistance of the product, H_2O. The 13X zeolite modification method was as follows. After mixing the 13X zeolite and 0.5 M HNO_3 in a ratio of 1 g of zeolite to 10 ml of HNO_3, the mixture was stirred in a water bath at 95 °C for 1 h. The modified support was filtered and washed thoroughly until the acid was completely removed and dried overnight before use. The modified zeolite support was designated as 13X-D.A (Si/Al = 1.91). The palladium nitrate precursor (1 wt%) was weighed and completely dissolved in distilled water, which was mixed with the zeolite and stirred as a slurry for approximately 1 h. Subsequently, the slurry was dried using an evaporator and calcined at 300 °C, 400 °C, 500 °C, and 600 °C for 4 h. The as-prepared catalysts were named Pd/13X(400), Pd/13X-DA(300), Pd/13X-DA(400), Pd/13X-DA(500), and Pd/13X-DA(600), respectively.

3.3. Characterizations

The sample was prepared by adding a small amount of catalyst powder to ethanol, followed by adding one drop of the mixed sample into the Cu grid using an ultrasonic vibrator. After drying, the temperature-programmed oxidation and reduction (TPOR) analysis was conducted to evaluate the dissociative hydrogen adsorption capacity of the catalyst. TPOR analysis was performed using an Autochem 2920 (Micrometrics). The TPOR analysis was carried out as follows: after the catalyst was filled, the oxygen species of the catalyst layer were fully adsorbed, while a gas mixture of O_2 and N_2 (5 : 95 vol/vol) was injected at 100 °C for 30 min. Subsequently, the temperature of the catalyst layer was reduced to 40 °C, and the physically adsorbed oxygen species were removed while injecting Ar. Finally, the H_2 concentration was measured using a thermal conductivity detector (TCD) over time, while injecting 500 ppm of H_2/N_2 gas. In addition, the crystal growth and structure of the as-prepared material were examined using XRD (Rigaku, D/MAX-2200 Ultima). The surface areas of the Ni-based catalysts used in this study were measured *via* physical nitrogen adsorption at −196 °C using an ASAP 2010 instrument (Micrometrics). The specific surface area was analyzed using the BET model. The dispersion and crystallite size of the catalysts were characterized *via* H_2 chemisorption at 35 °C using an Autochem 2920 (Micrometrics) instrument. The catalyst samples were activated with 10% H_2 at 300 °C for 0.5 min, cooled to 50 °C, and purged with He gas until the baseline was stable and saturated with H_2 pulses. Field emission transmission electron microscopy (TEM) analysis was performed to measure the crystal size of the active metal and support. A Tecnai G2 F30 S-Twin (FEI, USA) was used, and ZrO/W(100) Schottky emitter of the electron gun was applied.

3.4. Catalytic activity tests

The hydrogen oxidation test facility was a continuous-flow-type fixed-bed reactor, which consisted of a quartz tube with an inner diameter of 8 mm. Quartz wool was used to fix the catalyst layers. The gas supplied to the reactor was controlled using a mass flow controller (MFC, MKS Co.). The $H_2 : O_2 : N_2$ weight ratio of the gas mixture was 0.1–1.5 : 21 : 78.9–77.5 (vol/vol). The flow rate was adjusted to 1000 cm^3 min^{-1}. A cold trap (CTB-10, Jeiotech.) was used to collect water released after the reaction. A thermal conductivity analyzer (ZAFEK403 Fuji Elec. Co.) was used to analyze the unreacted H_2 in the injected gas and exhaust gas. The temperatures of the front and rear sides of

the catalyst layer were maintained using a K-type thermocouple during the reaction experiments. The temperature was measured using a thermometer (TM-721D TENMARS). The conversion rate of hydrogen was calculated by measuring the hydrogen concentration in the outlet after the reaction and in the inlet, as shown in the following equation:

$$\{(H_2, \text{inlet} - H_2, \text{outet})/H_2, \text{inlet}\} \times 100$$

4. Conclusions

In this study, the following results were obtained using Pd/zeolite-based catalysts to remove hydrogen from low concentrations (0.3%) to high concentrations (4%). When hydrogen oxidation reactions were performed, it was confirmed that the conversion rate of the catalysts decreased with the decrease in the hydrogen concentration. When the 13X zeolite was heat-treated at 400 °C, hydrogen oxidation of 95% or more was achieved even at a low hydrogen concentration (0.3%). The 1% Pd/13X zeolite D.A. catalyst exhibited an active particle diameter of 14.79 nm and a metal dispersion degree of 7.5755%. Therefore, the metal was highly dispersed on the catalyst surface. The 13X zeolite support was modified as an unstable structural state by disrupting the 13X zeolite structure and allowing Al_2O_3 to exist in an amorphous state. However, the improved dispersion degree of Pd *via* an acidic treatment on the surface was advantageous because of the structural effects of instability. In addition, the H_2-TPOR analysis confirmed that hydrogen was weakly adsorbed, and Pd had the ability to form hydride phases under normal conditions on the surface of the catalyst. Therefore, the performance improvement of the catalyst was determined by the improvement in the dispersion degree of Pd and the improvement in the control of the weak adsorption of hydrogen rather than the structural effects. In addition, it was confirmed that the moisture resistance of the support through hydrophobic modification prevented the adsorption of the product (H_2O) on the catalyst surface, thereby improving the hydrogen room temperature oxidation performance.

Author contributions

Younghee Jang: data curation, formal analysis, investigation, writing-original draft. Sang Moon Lee: investigation, writing-review & editing, supervision. Sung Su Kim: conceptualization, writing-review&editing, supervision.

Conflicts of interest

There are no conflicts to declare.

Acknowledgements

This work was supported by the Korea Agency for Infrastructure Technology Advancement (KAIA) grant funded by the Ministry of Land, Infrastructure and Transport (Grant 21CTAP-C157653-02).

Notes and references

1 H. T. Hwang, A. Al-Kukhun and A. Varma, *Int. J. Hydrogen Energy*, 2012, **37**, 2407–2411.
2 S. Satyapal, J. Petrovic, C. Read, G. Thomas and G. Ordaz, *Catal. Today*, 2007, **120**, 246–256.
3 D. Mori and K. Hirose, *Int. J. Hydrogen Energy*, 2009, **34**, 4569–4574.
4 S. Petrescu, C. Petre, M. Costea, O. Malancioiu, N. Boriaru, A. Dobrovicescu, M. Feidt and C. Harman, *Energy*, 2010, **35**, 729–739.
5 M. A. Hernández-Nochebuena, I. Cervantes and I. Araujo-Vargas, *Int. J. Hydrogen Energy*, 2021, **46**, 21160–21181.
6 H. Xing, C. Stuart, S. Spence and H. Chen, *Sustain*, 2021, **13**, 1–34.
7 J. Loy-Benitez, U. Safder, H. T. Nguyen, Q. Li, T. Y. Woo and C. K. Yoo, *Energy*, 2021, **233**, 121099.
8 H. Peng, J. Li, A. Thul, K. Deng, C. Ünlübayir, L. Löwenstein and K. Hameyer, *eTransportation*, 2020, **4**, 100057.
9 J. Kim, E. Jung and S. Kang, *Int. J. Hydrogen Energy*, 2015, **40**, 11762–11770.
10 Z. Xu and T. Jordan, *Int. J. Hydrogen Energy*, 2017, **42**, 7467–7473.
11 E. A. Reinecke, S. Kelm, W. Jahn, C. Jäkel and H. J. Allelein, *Int. J. Hydrogen Energy*, 2013, **38**, 8117–8124.
12 J. Yáñez, A. Kotchourko, A. Lelyakin, A. Gavrikov, A. Efimenko, M. Zbikowski, D. Makarov and V. Molkov, *Int. J. Hydrogen Energy*, 2011, **36**, 2613–2619.
13 W. Yu, X. Yu, S. T. Tu and P. Tian, *Int. J. Hydrogen Energy*, 2017, **42**, 14829–14840.
14 R. A. Molla, P. Bhanja, K. Ghosh, S. S. Islam, A. Bhaumik and S. M. Islam, *ChemCatChem*, 2017, **9**, 1939–1946.
15 L. Wang, H. Yue, Z. Hua, H. Wang, X. Li and L. Li, *Appl. Catal., B*, 2017, **219**, 301–313.
16 J. Mondal, A. Modak and A. Bhaumik, *J. Mol. Catal. A: Chem.*, 2011, **350**, 40–48.
17 T. Uda, M. Tanaka and K. Munakata, *Fusion Eng. Des.*, 2008, **83**, 1715–1720.
18 Y. Iwai, K. Sato and T. Yamanishi, *J. Plasma Fusion Res.*, 2010, **9**, 332–337.
19 Y. Iwai, K. Sato and T. Yamanishi, *Fusion Eng. Des.*, 2011, **86**, 2164–2167.
20 D. Łomot and Z. Karpiński, *Res. Chem. Intermed.*, 2015, **41**, 9171–9179.
21 G. J. Kim, J. H. Shin and S. Chang Hong, *Int. J. Hydrogen Energy*, 2020, **45**, 17276–17286.
22 M. Tanaka, T. Uda, Y. Shinozaki and K. Munakata, *Fusion Eng. Des.*, 2009, **84**, 1818–1822.
23 Y. Iwai, K. Sato, J. Taniuchi, H. Noguchi, H. Kubo, N. Harada, Y. Oshima and T. Yamanishi, *J. Nucl. Sci. Technol.*, 2011, **48**, 1184–1192.
24 C. Ramakrishna, B. K. Saini, K. Racharla, S. Gujarathi, C. S. Sridara, A. Gupta, G. Thakkallapalli, P. V. L. Rao, T. Uda, T. Sugiyama, Y. Asakura, K. Munakata, M. Tanaka,

K. Munakata, T. Uda, Y. Shinozaki, K. Munakata, D. Łomot, Z. Karpiński, S. A. Singh, K. Vishwanath, G. Madras, v. M. buyanov, D. Łomot, Z. Karpiński, M. T. Janicke, H. Kestenbaum, U. Hagendorf, F. Schüth, M. Fichtner and K. Schubert, *Pol. J. Chem. Technol.*, 2016, **18**, 15–18.

25 D. Łomot and Z. Karpiński, *Pol. J. Chem. Technol.*, 2016, **18**, 15–18.

26 E. Lalik, R. Kosydar, R. Tokarz-Sobieraj, M. Witko, T. Szumełda, M. Kołodziej, W. Rojek, T. Machej, E. Bielańska and A. Drelinkiewicz, *Appl. Catal., A*, 2015, **501**, 27–40.

27 M. T. Janicke, H. Kestenbaum, U. Hagendorf, F. Schüth, M. Fichtner and K. Schubert, *J. Catal.*, 2000, **191**, 282–293.

28 M. C. Silaghi, C. Chizallet, J. Sauer and P. Raybaud, *J. Catal.*, 2016, **339**, 242–255.

29 L. Luo, L. Zheng, X. Zhang, F. Jiang, L. Xia, J. Dai and D. Meng, *J. Solid State Chem.*, 2022, **305**, 122640.

30 N. Alimohammadi and S. Fathi, *React. Kinet., Mech. Catal.*, 2019, **128**, 949–964.

31 C. Ramakrishna, B. K. Saini, K. Racharla, S. Gujarathi, C. S. Sridara, A. Gupta, G. Thakkallapalli and P. V. L. Rao, *RSC Adv.*, 2016, **6**, 90720–90731.

32 B. A. Alshahidy and A. S. Abbas, *AIP Conf. Proc.*, 2020, **2213**, 020167.

33 L. E. Burris and M. C. G. Juenger, *Cem. Concr. Res.*, 2016, **79**, 185–193.

34 Y. Long, Y. Wang, H. Wu, T. Xue, P. Wu and Y. Guan, *RSC Adv.*, 2019, **9**, 25345–25350.

35 Y. Guo, G. Lu, Z. Zhang, S. Zhang, Y. Qi and Y. Liu, *Catal. Today*, 2007, **126**, 296–302.

36 M. Modelska, M. J. Binczarski, Z. Kaminski, S. Karski, B. Kolesinska, P. Mierczynski, C. J. Severino, A. Stanishevsky and I. A. Witonska, *Catalysts*, 2020, 444–466.

37 S. Bhogeswararao and D. Srinivas, *J. Catal.*, 2015, **327**, 65–77.

38 I. Friberg, A. H. Clark, P. H. Ho, N. Sadokhina, G. J. Smales, J. Woo, X. Auvray, D. Ferri, M. Nachtegaal, O. Kröcher and L. Olsson, *Catal. Today*, 2021, **382**, 3–12.

39 N. Y. Chen, *J. Phys. Chem.*, 1976, **80**, 60–64.

40 A. Bolshakov, N. Kosinov, D. E. Romero Hidalgo, B. Mezari, A. J. F. Van Hoof and E. J. M. Hensen, *Catal. Sci. Technol.*, 2019, **9**, 4239–4247.